

SDFed: Bridging Local–Global Discrepancy via Subspace Refinement and Divergence Control in Federated Prompt Learning

Yicheng Di*

Wei Yuan*

diyicheng1@stu.jiangnan.edu.cn
w.yuan@uq.edu.au
University of Queensland
Brisbane, Australia

Ao Ma

JD.com

Beijing, China

maaoaoma@126.com

Tieke He

Nanjing University
Nanjing, China
hetieke@gmail.com

Yuan Liu

Jiangnan University
Wuxi, China
lyuan1800@jiangnan.edu.cn

Zhanjie Zhang

Zhejiang University
Hangzhou, China
cszzj@zju.edu.cn

Hongzhi Yin†‡

University of Queensland
Brisbane, Australia
h.yin1@uq.edu.au

Abstract

Vision-language pretrained models (VLPMs) offer strong transferable representations, yet adapting them in privacy-sensitive multi-party settings is challenging due to the high communication cost of federated optimization and the limited local data on clients. Federated prompt learning mitigates this issue by keeping the VLPM backbone frozen and collaboratively training lightweight prompt parameters. However, existing approaches typically enforce a unified prompt structure and length across clients, which is inadequate under practical client heterogeneity in both data distributions and system resources, and may further introduce conflicts between globally shared and locally optimal knowledge.

To address these challenges, we propose **SDFed**, a heterogeneous federated prompt learning framework that bridges Local–Global Discrepancy via Subspace Refinement and Divergence Control. SDFed maintains a fixed-length global prompt for efficient aggregation while allowing each client to learn a variable-length local prompt to better match its data characteristics and capacity. To mitigate local–global conflicts and facilitate effective knowledge transfer, SDFed introduces a subspace refinement method for local prompts and an information retention and divergence control strategy that preserves key local information while maintaining appropriate separability between global and local representations. Extensive experiments on several datasets demonstrate that SDFed consistently improves performance and robustness in heterogeneous federated settings.

*Both authors contributed equally to this research.

†‡ is the corresponding author.

Permission to make digital or hard copies of all or part of this work for personal or classroom use is granted without fee provided that copies are not made or distributed for profit or commercial advantage and that copies bear this notice and the full citation on the first page. Copyrights for components of this work owned by others than the author(s) must be honored. Abstracting with credit is permitted. To copy otherwise, or republish, to post on servers or to redistribute to lists, requires prior specific permission and/or a fee. Request permissions from permissions@acm.org.

XX, Woodstock, NY

© 2018 Copyright held by the owner/author(s). Publication rights licensed to ACM.

ACM ISBN 978-1-4503-XXXX-X/18/06

<https://doi.org/XXXXXX.XXXXXXX>

The code is available at <https://anonymous.4open.science/r/SDFed-F324>.

CCS Concepts

• Computing methodologies → Distributed algorithms.

Keywords

Heterogeneous Federated Learning, VLPMs, Subspace Refinement

ACM Reference Format:

Yicheng Di, Wei Yuan, Tieke He, Zhanjie Zhang, Ao Ma, Yuan Liu, and Hongzhi Yin†‡. 2018. SDFed: Bridging Local–Global Discrepancy via Subspace Refinement and Divergence Control in Federated Prompt Learning. In *Proceedings of Make sure to enter the correct conference title from your rights confirmation email (XX)*. ACM, New York, NY, USA, 13 pages. <https://doi.org/XXXXXX.XXXXXXX>.

1 Introduction

Vision-language pretrained models (VLPMs), exemplified by Contrastive Language-Image Pretraining (CLIP) [37], have become a strong foundation for a wide range of vision-language tasks. Meanwhile, many real-world applications require multiple parties to collaboratively adapt such powerful pretrained models while keeping raw data local due to privacy constraints, making federated learning (FL) an increasingly important paradigm [23, 25]. However, mainstream FL pipelines typically rely on frequent exchanges of model parameters between clients and a central server [45]. Directly bringing large VLPMs into federated optimization substantially amplifies communication overhead, and it may also aggravate overfitting when each client has limited local data.

Prompt learning is a parameter-efficient adaptation paradigm that keeps the pretrained backbone frozen and optimizes only a small set of additional prompt parameters [51], which has been widely used in centralized VLPM optimization. This naturally leads to federated prompt learning, where clients collaboratively train prompts while avoiding the costly transmission of the whole backbone. Existing federated prompt learning methods often follow

the classical FedAvg-style aggregation [30]: clients locally optimize prompt parameters and the server aggregates them into a shared global prompt. Representative examples include PromptFL [14], which enables clients to jointly learn soft prompts without updating the entire model.

Despite this progress, current federated prompt learning remains limited when facing client heterogeneity, which is prevalent in real-world deployments. As illustrated in Fig.1, clients may differ substantially in both data distributions (non-IID) and system conditions such as model architectures and available computational resources [41, 49]. Most existing approaches assume that all clients share prompts with an identical structure and length, and synchronize only a single global prompt across clients. This design makes it difficult to adapt prompt representations to diverse local data complexity and client model capacity [46, 50]. Moreover, even when a global prompt provides a shared representation with certain generalization ability, it can introduce information that conflicts with locally optimal features for some clients, impairing local convergence and limiting personalization performance [21, 24, 28, 32]. Although more recent efforts leverage prompts to encode task-specific key information and to alleviate the performance degradation caused by non-IID data, e.g., UOPP [29] and prompt-driven prototype update mechanisms [8, 57], they still generally use a single same prompt across clients. Under highly non-IID distributions and heterogeneous model architectures, different clients may prefer different discriminative subspaces [3, 27], making simple statistical averaging of a single global prompt insufficient to serve all clients well.

These observations motivate us to explore heterogeneous federated prompt learning, where prompt structures and lengths are allowed to vary across clients to adapt to diverse local data characteristics and system resources. However, enabling such heterogeneity introduces two fundamental challenges. First, to better capture client-specific data distributions and model capacities, different clients should employ prompt vectors of different lengths [29, 54]. Meanwhile, due to communication constraints, the server can only access and aggregate uploaded prompt parameters in a unified manner. This leads to **CH1: How can we adaptively assign heterogeneous prompt lengths to different clients while preserving global aggregability under limited server access?** Second, when global prompts and local prompts coexist, their learned knowledge may conflict. Specifically, globally shared representations may not always align with locally optimal features, while excessive local optimization may hinder effective cross-client knowledge transfer. This gives rise to **CH2: How can we resolve local-global knowledge conflicts while facilitating efficient knowledge transfer in heterogeneous federated prompt learning?**

To address these challenges, we propose **SDFed**, which bridges Local-Global Discrepancy via Subspace Refinement and Divergence Control in federated prompt learning. SDFed first establishes a Prompt-Driven Federated Heterogeneous Framework to coordinate diverse prompt requirements across clients (addressing **CH1**). Specifically, each client maintains a global prompt of uniform length and a local prompt with a unique length, and they are implicitly linked through shared tokens and a frozen encoder to ensure both aggregability and personalization. To mitigate local-global conflicts (addressing **CH2**), SDFed introduces a Subspace Refinement method for local prompts that filters conflicting components while

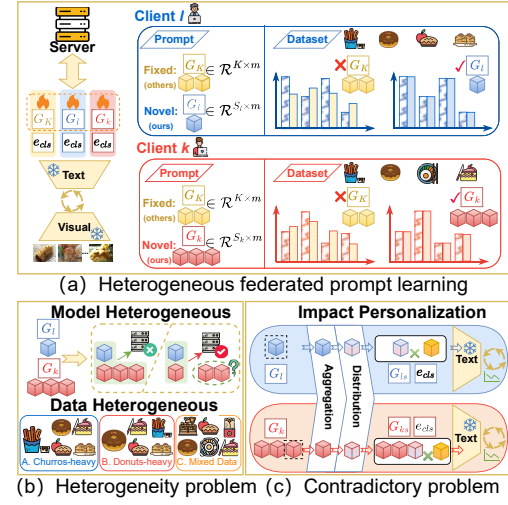


Figure 1: Challenges in prompt-driven federated framework.

preserving key local information. In addition, an Information Retention and Divergence Control strategy maintains consistency between local features and their projections while enforcing separability between global and local representations, achieving a balance between information fidelity and personalization.

We summarize our main contributions as follows: (1) We propose SDFed, a federated prompt learning framework tailored for data and model heterogeneity, with an explicit focus on resolving conflicts between global and local knowledge. (2) We develop a Subspace Refinement method for local prompts together with an Information Retention and Divergence Control strategy to remove local-global conflicts while preserving key local information and maintaining representation distinctiveness. (3) Extensive experiments on single-domain, multi-domain, and classical image datasets demonstrate that SDFed achieves superior performance and robustness in heterogeneous environments.

2 Related Work

2.1 Heterogeneity in Federated Learning

Heterogeneity within federated learning remains a major obstacle to model performance and generalization [34, 43]. Recent studies have sought to mitigate performance degradation caused by disparities in data, models, and systems. HiCS-FL [5] and FedGNSR [40] address non-IID data by modeling and clustering client distributions, while FedLMT [26] employs low-rank sub-model training to enable efficient optimization for resource-limited clients. FedIIIH [48] models both inter-client and intra-client heterogeneity through a hierarchical variational framework, and FedTA [47] introduces a Tail Anchor mechanism to improve spatiotemporal robustness in federated continual learning. Moreover, HtFLlib [52] provides the first standardized benchmark for heterogeneous federated learning. Despite these advances, the trade-off between personalization and generalization remains unresolved, as enhanced adaptability often undermines global consistency and convergence stability.

2.2 Federated Prompt Learning

Federated prompt learning has gained significant attention for enabling personalized collaboration with efficient parameter and communication usage [7, 13, 44]. In vision and language pre-trained models, CoOp [56] learns prompt contexts as vectors while keeping the backbone parameters fixed, achieving efficient adaptation for CLIP-like architectures. Powder [35] employs prompts as knowledge carriers in federated continual learning to enhance transfer and mitigate forgetting. FedOTP [22] jointly learns global and local prompts through unbalanced optimal transport to address distribution shifts and balance objectives. GPT-FL [55] utilizes generative pre-trained models with prompt-guided synthetic data to improve robustness, while UOPP [29] adopts task-wise prompt learning with adaptive dual heads to reduce interference and overfitting. Despite these advancements, current approaches remain constrained by architectural rigidity, facing difficulties in adapting to variable local prompt lengths and lacking a unified mechanism to disentangle conflicting global and local knowledge, which limits collaborative personalization. Unlike previous federated prompt learning methods that rely on fixed-length global prompts or simple local-global prompt separation, we propose SDFed, a unified framework tailored to client heterogeneity. SDFed adapts prompt length and mitigates local-global knowledge conflicts by allocating differentiated prompts to heterogeneous clients while preserving global aggregability, achieving more stable and personalized federated optimization through subspace refinement and divergence control.

3 Methodology

3.1 Preliminary

We summarize the frequently used notations in Appendix A. Prompt learning equips the CLIP text encoder with trainable parameters, allowing adaptation to downstream tasks while keeping the image encoder frozen. In contrast to zero-shot transfer that relies on hand-crafted templates (e.g., “an image depicting <label>”) and fixed word embeddings $V = v_1, \dots, v_c$, it learns continuous context vectors $G_e = g_1, \dots, g_S \in \mathcal{R}^{S \times m}$, where S is the prompt length and m the embedding dimension. Thus, each class label embedding e_{la} is embedded into a prompt-augmented textual input by combining it with the learnable context.

$$\tilde{F}_g = \{e_{st}, G_e, e_1, e_2, \dots, e_K, e_{la}, e_{en}\}, \quad (1)$$

where e_{st} and e_{en} are trainable start and end embeddings, $\{e_1, \dots, e_K\}$ are fixed word embeddings, and e_{la} is the class label embedding. The Transformer-based text encoder $s(\cdot)$ produces the prompt-aware text feature $\tilde{s}_g = s(\tilde{F}_g, \phi_s) \in \mathcal{R}^m$, where ϕ_s contains frozen pre-trained weights and learnable prompt parameters G_e . For classification, we compare class-specific text features $\{\tilde{s}_{gi}\}_{i=1}^L$ with the image feature $\tilde{d} = d(q)$ from the frozen image encoder and compute the probability of class h via their similarity:

$$G(\hat{p} = h | q) = \frac{\exp(\text{sim}(\tilde{s}_{gh}, \tilde{d}) / \mu)}{\sum_{l=1}^L \exp(\text{sim}(\tilde{s}_{gl}, \tilde{d}) / \mu)}, \quad (2)$$

where $\text{sim}(\cdot)$ represents the cosine similarity, and μ serves as a temperature parameter that regulates the smoothness of the softmax distribution. The learnable prompt parameters G_e are optimized

using the cross-entropy loss. For the dataset Ω composed of input–output pairs (Q, p) , the optimization objective is defined as:

$$\mathcal{L}_{ce} = \arg \min_{G_e} \mathbb{E}_{(Q, p) \sim \Omega} \mathcal{L}(\text{sim}(\tilde{s}_g, \tilde{d}), p). \quad (3)$$

3.2 Prompt-Driven Federated Heterogeneous Framework

In federated learning, heterogeneous client data and objectives make a single fixed-length prompt inadequate for both personalization and global aggregation. We therefore propose a Prompt Driven Federated Heterogeneous Framework with a fixed-length shared global prompt for consistency and a variable-length client-specific local prompt for personalization in Fig. 2. Consider M clients and a central server. Client l holds a local dataset Ω_l of size h_l , and in round z a subset \mathbb{S}_z participates, each running O local epochs to minimize \mathcal{L} . Each client maintains a fixed-length global prompt $G_{s,l}^{z,o} \in \mathcal{R}^{S_s \times m}$ and a variable-length local prompt $G_{c,l}^{z,o} \in \mathcal{R}^{S_{c,l} \times m}$, which are jointly updated at step o with learning rate β as:

$$G_{*,l}^{z,o+1} = G_{*,l}^{z,o} - \beta \nabla_{G_{*,l}} \mathcal{L}(G_{s,l}^{z,o}, G_{c,l}^{z,o}; \Omega_l), \quad (4)$$

where $G_{*,l}^{z,o} \in \{G_{s,l}^{z,o}, G_{c,l}^{z,o}\}$. After local training, client l uploads only the global prompt $G_{s,l}^{z,O}$ for server aggregation and keeps $G_{c,l}^{z,O}$ private for personalization. The server aggregates $G_{s,l}^{z,O}$ via a sample size weighted average with weights proportional to h_l :

$$G_s^{(z+1,0)} = \sum_{l \in \mathbb{S}_z} \frac{h_l}{\sum_{k \in \mathbb{S}_z} h_k} G_{s,l}^{z,O}, \quad (5)$$

where h_l is the size of Ω_l , so clients with more data contribute more to aggregation. The updated global prompt $G_s^{(z+1,0)}$ is then broadcast to all clients to initialize the next round. Formally, the objective is:

$$\min_{G_s, \{G_{c,l}\}_{l=1}^M} \sum_{l=1}^M \frac{h_l}{\sum_{k=1}^M h_k} \mathcal{L}_l(G_{s,l}^{z,o}, G_{c,l}^{z,o}; \Omega_l), \quad (6)$$

where $\mathcal{L}_l(\cdot)$ is the loss of client l on Ω_l . We jointly optimize global and local prompts during training, but use only the local-prompt features for inference to adapt to each client’s data and preserve personalization. Unlike existing methods, we couple a fixed-length global prompt with a variable-length client-specific local prompt. For structural alignment, we set the maximum prompt length across clients and use frozen tokens $e_{st}, e_{la}, e_{su}, e_{en}$. Each client concatenates its prefix, class, and suffix tokens with the global prompt $G_{s,l}^{z,o}$, the local prompt $G_{c,l}^{z,o}$, and the projected local prompt $\tilde{G}_{c,l}^{z,o}$ (see Eq. (10)). If the sequence is shorter than K_{\max} , zero-padding tokens e_{pa} are appended. The resulting input sequence is:

$$\tilde{F}_g = \{e_{st}, G_e, e_{la}, e_{su}, e_{en}, e_{pa}\}, \quad (7)$$

Global and local prompts share prefix and suffix tokens and the same Transformer encoder, enabling joint learning in a unified space while preserving client-specific local information. The resulting text features are matched with frozen CLIP image features to compute similarities for classification.

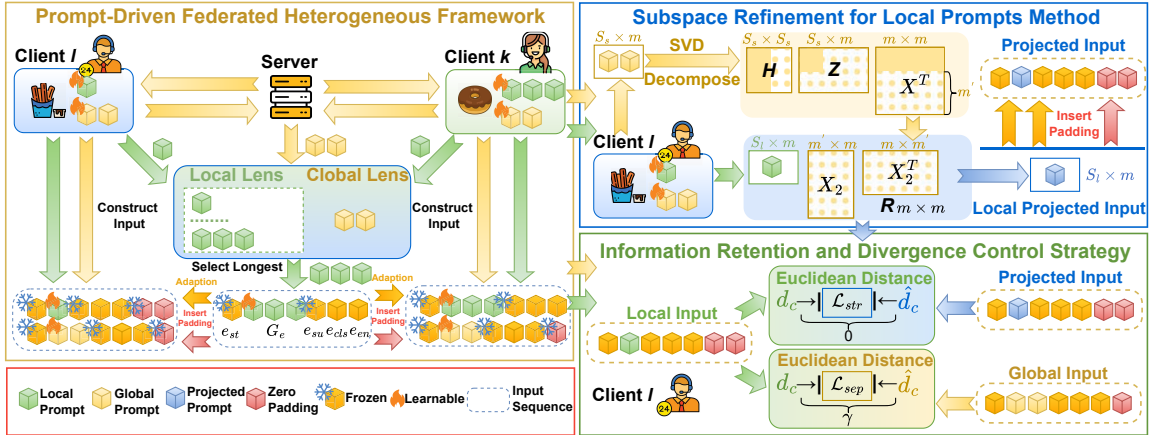


Figure 2: Our proposed SDFed comprises three modules: The Prompt-Driven Federated Heterogeneous Framework assigns each client a variable-length local prompt and a shared global prompt. The Subspace Refinement for Local Prompts Method projects local prompts onto a global-derived subspace to mitigate conflicts. The Information Retention and Divergence Control Strategy aligns local and refined features while enforcing separation from global features, using only local features at inference.

3.3 Subspace Refinement for Local Prompts Method

While separating global and local prompts enables personalization via prompt-length heterogeneity, strong client heterogeneity still demands explicit interaction to avoid semantic conflicts that simple alignment or orthogonality constraints cannot resolve. We therefore refine each local prompt by projecting it onto a subspace that suppresses components dominated by the global prompt. Specifically, for the global prompt $G_s^{z,o} \in \mathcal{R}^{S_s \times m}$ at step o of round z , we perform SVD:

$$G_s^{z,o} = HZX^T, \quad (8)$$

In the singular value decomposition, $H \in \mathcal{R}^{S_s \times S_s}$ and $X \in \mathcal{R}^{m \times m}$ are the left and right singular matrices, and $Z \in \mathcal{R}^{S_s \times m}$ contains singular values in descending order. Since $S_s \neq S_l$, we construct the projection in the shared embedding space using X , whose dimension m matches the embedding dimension of both prompts. Let $X_2 \in \mathcal{R}^{m \times m'}$ collect the columns of X corresponding to the smaller singular values, and let m' be determined by the ratio λ :

$$m' = \lfloor (1 - \lambda)m \rfloor, \quad (9)$$

where $\lfloor \cdot \rfloor$ denotes rounding down.

DEFINITION 1 (EFFECTIVE NULL-SPACE DIMENSION CONTROLLED BY λ). Let σ_i be the singular values of $G_s^{z,o}$ and $X = [x_1, \dots, x_m]$ the right-singular matrix. We select $X_2 = [x_{\lfloor \lambda m \rfloor + 1}, \dots, x_m] \in \mathcal{R}^{m \times m'}$, with m' as the effective null-space dimension. The hyperparameter $\lambda \in (0, 1)$ controls how many dominant global directions (top $\lfloor \lambda m \rfloor$ right-singular vectors) are excluded from the local prompt update.

We construct the projection matrix $R^{z,o} = X_2 X_2^T$ and obtain:

$$\tilde{G}_{c,l}^{z,o} = G_{c,l}^{z,o} R^{z,o} = G_{c,l}^{z,o} X_2 X_2^T, \quad (10)$$

where $G_{c,l}^{z,o} \in \mathcal{R}^{S_l \times m}$ is client l 's local prompt and $\tilde{G}_{c,l}^{z,o} \in \mathcal{R}^{S_l \times m}$ is its projection with the same shape.

LEMMA 1 (SPECTRAL FILTERING INTERPRETATION OF λ). Let $R^{z,o} = X_2 X_2^T$ and $\tilde{G}_{c,l}^{z,o} = G_{c,l}^{z,o} R^{z,o}$. Then $R^{z,o}$ is the orthogonal projector onto $\text{span}(X_2)$, removing components of $G_{c,l}^{z,o}$ along the top $\lfloor \lambda m \rfloor$ right-singular directions of $G_s^{z,o}$, while retaining the remaining m' directions.

The top right-singular directions of $G_s^{z,o}$ capture shared global semantics, while the remaining ones encode weaker or client-specific variations. Projecting $G_{c,l}^{z,o}$ onto $\text{span}(X_2)$ suppresses components aligned with dominant global directions, reducing redundancy and global-local interference. The proofs are in Appendix C.1 and C.5.

THEOREM 1 (OPTIMALITY OF NULL-SUBSPACE REFINEMENT). For round-step pair (z, o) , let $R^{z,o} = X_2 X_2^T$ be the orthogonal projector. For any client l 's local prompt $G_{c,l}^{z,o}$, the refined prompt $\tilde{G}_{c,l}^{z,o} := G_{c,l}^{z,o} R^{z,o}$ is the unique solution to the constrained least-squares problem

$$\tilde{G}_{c,l}^{z,o} = \arg \min_U \|U - G_{c,l}^{z,o}\|_F^2 \text{ s.t. } U = UR^{z,o}. \quad (11)$$

Equivalently, $\tilde{G}_{c,l}^{z,o}$ is the closest matrix to $G_{c,l}^{z,o}$ whose row-space lies in $\text{span}(X_2)$, preserving only the truncated global directions.

3.4 Information Retention and Divergence Control Strategy

To mitigate global-local conflicts, we project the local prompt $G_{c,l}^{z,o}$ onto its null-space, which may discard some client-specific information. We therefore propose an Information Retention and Divergence Control Strategy: the stretch term aligns $G_{c,l}^{z,o}$ with its projection to preserve semantics, while the separate term enforces sufficient divergence from the global prompt. Concretely, we minimize the MSE between $d(G_{c,l}^{z,o})$ and $d(\tilde{G}_{c,l}^{z,o})$:

$$\mathcal{L}_{str} = \|d(G_{c,l}^{z,o}) - d(\tilde{G}_{c,l}^{z,o})\|_2^2, \quad (12)$$

This mechanism guides $G_{c,l}^{z,o}$ to gradually stretch toward its null space projection $\tilde{G}_{c,l}^{z,o}$, preserving key semantics while removing

Algorithm 1 Overall Procedure of SDFed.

Input: Rounds B , clients $\{1, \dots, M\}$ with datasets $\{\Omega_l\}$ and sizes $\{h_l\}$, local steps O , init global prompt G_s^0 , init local prompts $\{G_{c,l}^0\}$, step size β , margin γ .

Output: Final client prompts $\{(G_s^B, G_{c,l}^B)\}_{l=1}^M$.

- 1: **Server:** initialize G_s^0
- 2: **for** $z = 0, 1, \dots, B-1$ **do**
- 3: Sample participating clients \mathbb{S}_z and broadcast G_s^z to $l \in \mathbb{S}_z$
- 4: **for** $l \in \mathbb{S}_z$ in parallel **do**
- 5: $(G_{s,l}^{z,O}, G_{c,l}^{z,O}) \leftarrow \text{LOCALUPDATE}(G_s^z, G_{c,l}^z, \Omega_l)$
- 6: Upload only $G_{s,l}^{z,O}$
- 7: **end for**
- 8: Aggregate $G_s^{z+1} \leftarrow \sum_{l \in \mathbb{S}_z} \frac{h_l}{\sum_{k \in \mathbb{S}_z} h_k} G_{s,l}^{z,O}$ ▷ By Eq. (5)
- 9: Set $G_{c,l}^{z+1} \leftarrow G_{c,l}^{z,O}$ for $l \in \mathbb{S}_z$
- 10: **end for**
- 11: **return** $\{(G_s^B, G_{c,l}^B)\}_{l=1}^M$
- 12: LOCALUPDATE(G_s , G_c , Ω_l):
- 13: **for** $o = 0, 1, \dots, O-1$ **do**
- 14: Compute SVD $G_s = HZ\mathbf{X}_2^\top$ and set $R = \mathbf{X}_2\mathbf{X}_2^\top$ with $\mathbf{X}_2 = [x_{[\lambda m]+1}, \dots, x_m]$ ▷ By Eqs. (8–10)
- 15: $\tilde{G}_c \leftarrow G_c R$ ▷ By Eq. (10)
- 16: $\mathcal{L} \leftarrow \mathcal{L}_{ce}(G_c; \Omega_l) + \mathcal{L}_{ce}(G_s; \Omega_l) + \|d(G_c) - d(\tilde{G}_c)\|_2^2 + \text{ReLU}(\gamma - \|d(G_c) - d(G_s)\|_2)$ ▷ By Eq. (14)
- 17: $G_s \leftarrow G_s - \beta \nabla_{G_s} \mathcal{L}$, $G_c \leftarrow G_c - \beta \nabla_{G_c} \mathcal{L}$ ▷ By Eq. (4)
- 18: **end for**
- 19: **return** (G_s, G_c)

features that conflict with the global prompt. To avoid excessive convergence toward the global prompt, a separate term with a margin constraint is added to maintain a proper distance between $d(G_{c,l}^{z,O})$ and $d(G_s^{z,O})$. It is formally defined as:

$$\mathcal{L}_{sep} = \text{ReLU}(\gamma - \|d(G_{c,l}^{z,O}) - d(G_s^{z,O})\|_2), \quad (13)$$

where γ ensures each local prompt preserves personalization without excessive influence from the global prompt. During training, the MSE-based stretch and separate terms, along with the cross-entropy loss on local and global prompts, form the unified objective:

$$\mathcal{L} = \mathcal{L}_{ce}(G_{c,l}^{z,O}, p_l) + \mathcal{L}_{ce}(G_s^{z,O}, p_l) + \mathcal{L}_{str} + \mathcal{L}_{sep}, \quad (14)$$

This strategy mitigates conflicts from data heterogeneity, allowing local prompts to preserve discriminative representations while leveraging shared global knowledge. The detailed workflow of SDFed is elaborated in Algorithm 1.

3.5 Convergence Analysis

Let client l have data distribution Ω_l with sample size h_l , and define weights $w_l = \frac{h_l}{\sum_{k=1}^M h_k}$. Denote the per-sample cross-entropy loss based on CLIP similarity in Eq. (2) as $\ell_{ce}(\cdot)$. The expected local objective for client l , corresponding to Eq. (14), is:

$$f_l(G_s, G_{c,l}) = \mathbb{E}_{(Q,p) \sim \Omega_l} [\mathcal{L}_{ce}(G_{c,l}, p) + \mathcal{L}_{ce}(G_s, p)] + \mathcal{L}_{str,l} + \mathcal{L}_{sep,l}, \quad (15)$$

where $\mathcal{L}_{str,l}$ and $\mathcal{L}_{sep,l}$ are from Eq. (12)–(13), and the projection $\tilde{G}_{c,l}^{z,O} = G_{c,l}^{z,O} R^{z,O} = \mathbf{X}_2 \mathbf{X}_2^\top$, with \mathbf{X}_2 from the SVD of $G_s^{z,O}$

and truncation ratio λ . The global objective is:

$$F(G_s, \{G_{c,l}\}_{l=1}^M) = \sum_{l=1}^M w_l f_l(G_s, G_{c,l}). \quad (16)$$

The algorithm performs O local steps on each selected client and aggregates the uploaded global prompts by Eq. (5).

ASSUMPTION 1 (L-SMOOTH). For each client l , $f_l(G_s, G_{c,l})$ is differentiable and L -smooth in both arguments, i.e.,

$$\|\nabla f_l(U) - \nabla f_l(V)\|_F \leq L \|U - V\|_F, \quad (17)$$

for any feasible U, V .

ASSUMPTION 2 (UNBIASED STOCHASTIC GRADIENTS AND BOUNDED VARIANCE). Let $g_{s,l}^{z,O}$ and $g_{c,l}^{z,O}$ be stochastic gradients of f_l w.r.t. G_s and $G_{c,l}$ computed from mini-batches. They are unbiased and satisfy:

$$\mathbb{E}[g_{s,l}^{z,O}] = \nabla_{G_s} f_l, \quad \mathbb{E}[g_{c,l}^{z,O}] = \nabla_{G_{c,l}} f_l, \quad (18)$$

where $\mathbb{E}\|g_{s,l}^{z,O} - \nabla_{G_s} f_l\|_F^2 \leq \sigma^2$, $\mathbb{E}\|g_{c,l}^{z,O} - \nabla_{G_{c,l}} f_l\|_F^2 \leq \sigma^2$.

ASSUMPTION 3 (CLIENT HETEROGENEITY). There exists $\delta \geq 0$ such that for all z and all l , we have:

$$\|\nabla_{G_s} f_l(G_s^{z,O}, G_{c,l}^{z,O}) - \nabla_{G_s} F(G_s^{z,O}, \{G_{c,k}^{z,O}\})\|_F^2 \leq \delta^2. \quad (19)$$

ASSUMPTION 4 (PROJECTION BOUNDEDNESS). For each (z, o) , the matrix $R^{z,O} = \mathbf{X}_2 \mathbf{X}_2^\top$ is a symmetric idempotent projector with $\|R^{z,O}\|_2 \leq 1$. This follows because \mathbf{X}_2 has orthonormal columns from the SVD, making $R^{z,O}$ an orthogonal projector.

We state the property of the null-space projection used in Eq. (10).

LEMMA 2 (NON-EXPANSIVENESS OF THE SUBSPACE REFINEMENT). For any matrix $A \in \mathcal{R}^{S_1 \times m}$ and any projector $R^{z,O}$ in Assumption 4, $\|AR^{z,O}\|_F \leq \|A\|_F$ and $\|A - AR^{z,O}\|_F \leq \|A\|_F$.

LEMMA 3 (SMOOTHNESS OF THE ADDITIONAL REGULARIZERS). Under Assumptions 1–4, the stretch and separate terms in Eq. (12)–(13) preserve L -smoothness: there exists $L' = \Theta(L)$ such that each f_l in Eq. (15) is L' -smooth.

LEMMA 4 (GRADIENT BOUNDEDNESS OF REGULARIZERS). Assume $d(\cdot)$ is L_d -Lipschitz in Frobenius norm, i.e., $\|d(A) - d(B)\|_2 \leq L_d \|A - B\|_F$. Then for each client l , $\|\nabla_{G_{c,l}} \mathcal{L}_{str}\|_F \leq 2L_d^2 \|G_{c,l}^{z,O} - \tilde{G}_{c,l}^{z,O}\|_F$, and \mathcal{L}_{sep} has a subgradient g with $\|g\|_F \leq L_d$ when $\mathcal{L}_{sep} > 0$.

Lemma 3 follows from: (i) Lemma 2 shows the projection is non-expansive, and (ii) the 1-Lipschitz property of $\text{ReLU}(\cdot)$, making \mathcal{L}_{sep} Lipschitz. We provide a stationarity bound for the global prompt sequence in Eq. (4)–(5). The proofs are in Appendix C.2–C.4.

THEOREM 2 (CONVERGENCE TO A FIRST-ORDER STATIONARY POINT). Suppose Assumptions 1–4 hold, and each client performs O local SGD steps with step size $\beta \leq \frac{1}{4L' O}$, where L' is from Lemma 3. Let Z be the number of communication rounds, and assume full participation (i.e., $\mathbb{S}_z = \{1, \dots, M\}$; partial participation follows similarly). Then the aggregated global prompts $\{G_s^{(z,O)}\}_{z=0}^{Z-1}$ satisfy:

$$\frac{1}{Z} \sum_{z=0}^{Z-1} \mathbb{E} \left\| \nabla_{G_s} F(G_s^{(z,O)}, \{G_{c,l}^{(z,O)}\}) \right\|_F^2 \leq \frac{2(F_0 - F_\star)}{\beta Z O} + \frac{4\beta L' \sigma^2}{M} + 8\beta^2 L'^2 O^2 \delta^2, \quad (20)$$

where $F_0 = F(G_s^{(0,0)}, \{G_{c,l}^{(0,0)}\})$ and $F_\star = \inf F$.

Table 1: Comparison in the single-domain scenarios. The highest test accuracy is highlighted in bold.

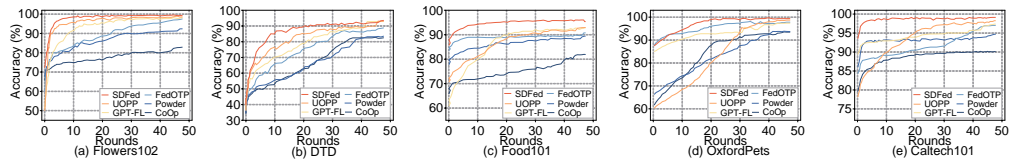
Method	Flowers102		DTD		Food101		OxfordPets		Caltech101	
	ViT-B16	ResNet50								
CoOp	83.23 \pm 0.65	78.45 \pm 0.82	82.91 \pm 2.14	75.12 \pm 2.45	81.65 \pm 2.31	76.84 \pm 2.56	93.41 \pm 1.29	88.52 \pm 1.45	90.36 \pm 0.52	85.64 \pm 0.78
Powder	92.46 \pm 0.53	88.12 \pm 0.64	83.23 \pm 2.95	76.54 \pm 3.12	88.41 \pm 0.52	83.21 \pm 0.75	93.76 \pm 0.42	89.15 \pm 0.62	94.75 \pm 0.61	90.12 \pm 0.84
FedOTP	97.51 \pm 0.12	92.34 \pm 0.25	89.84 \pm 0.25	82.15 \pm 0.42	90.71 \pm 0.11	85.67 \pm 0.31	97.54 \pm 0.13	92.45 \pm 0.24	97.02 \pm 0.05	92.15 \pm 0.18
GPT-FL	98.27 \pm 0.36	94.15 \pm 0.42	92.86 \pm 0.36	86.42 \pm 0.51	92.85 \pm 0.23	88.34 \pm 0.45	97.38 \pm 0.36	93.67 \pm 0.48	97.58 \pm 0.35	93.45 \pm 0.41
UOPP	98.62 \pm 1.34	95.21 \pm 1.45	93.09 \pm 0.42	87.56 \pm 0.62	92.94 \pm 0.18	89.12 \pm 0.34	98.71 \pm 0.21	94.82 \pm 0.35	98.24 \pm 0.31	94.78 \pm 0.52
SDFed	99.35\pm0.07	96.84\pm0.15	93.56\pm0.18	89.45\pm0.28	96.38\pm0.06	92.15\pm0.12	99.36\pm0.07	96.54\pm0.14	99.12\pm0.11	96.08\pm0.21

Table 2: Comparison in the OfficeHome. The table reports both the overall accuracy and the average accuracy for each domain.

Method	Product		Clipart		Real-World		Art		Avg	
	ViT-B16	ResNet50	ViT-B16	ResNet50	ViT-B16	ResNet50	ViViT-B16T	ResNet50	ViT-B16	ResNet50
CoOp	92.37 \pm 0.25	86.42 \pm 0.51	69.26 \pm 0.61	62.15 \pm 0.94	90.57 \pm 0.34	84.31 \pm 0.68	85.32 \pm 0.42	78.64 \pm 0.75	84.38 \pm 0.41	77.88 \pm 0.72
Powder	95.27 \pm 0.18	89.65 \pm 0.42	74.25 \pm 0.52	68.12 \pm 0.74	92.35 \pm 0.25	86.54 \pm 0.48	87.86 \pm 0.31	81.42 \pm 0.55	87.43 \pm 0.32	81.43 \pm 0.55
FedOTP	95.81 \pm 0.15	90.12 \pm 0.35	74.54 \pm 0.42	68.51 \pm 0.62	92.39 \pm 0.21	86.72 \pm 0.44	87.69 \pm 0.35	81.35 \pm 0.52	87.61 \pm 0.28	81.68 \pm 0.48
GPT-FL	94.75 \pm 0.22	88.34 \pm 0.41	76.32 \pm 0.45	70.21 \pm 0.58	89.75 \pm 0.31	83.56 \pm 0.45	82.27 \pm 0.41	76.12 \pm 0.62	85.77 \pm 0.35	79.56 \pm 0.52
UOPP	95.24 \pm 0.15	90.52 \pm 0.31	77.16 \pm 0.41	71.34 \pm 0.64	92.91 \pm 0.25	87.12 \pm 0.41	87.45 \pm 0.32	81.56 \pm 0.55	88.19 \pm 0.28	82.64 \pm 0.48
SDFed	95.82\pm0.11	91.45\pm0.24	78.48\pm0.32	73.56\pm0.45	93.23\pm0.14	88.14\pm0.32	88.64\pm0.21	83.12\pm0.44	89.04\pm0.20	84.07\pm0.36

Table 3: Comparison in the Office31. The table reports both the overall accuracy and the average accuracy for each domain.

Method	Webcam		Amazon		DSLR		Avg	
	ViT-B16	ResNet50	ViT-B16	ResNet50	ViT-B16	ResNet50	ViT-B16	ResNet50
CoOp	81.72 \pm 0.41	75.34 \pm 0.82	85.61 \pm 0.32	79.45 \pm 0.65	78.52 \pm 0.55	72.18 \pm 0.91	81.95 \pm 0.43	75.66 \pm 0.79
Powder	90.25 \pm 0.35	84.18 \pm 0.52	89.19 \pm 0.24	83.42 \pm 0.41	85.94 \pm 0.48	80.21 \pm 0.67	88.46 \pm 0.36	82.60 \pm 0.53
FedOTP	91.32 \pm 0.25	85.42 \pm 0.44	89.43 \pm 0.21	83.86 \pm 0.38	86.14 \pm 0.32	80.65 \pm 0.55	88.96 \pm 0.26	83.31 \pm 0.46
GPT-FL	94.43 \pm 0.32	89.15 \pm 0.48	90.51 \pm 0.25	85.12 \pm 0.34	88.39 \pm 0.31	82.74 \pm 0.51	91.11 \pm 0.29	85.67 \pm 0.44
UOPP	94.61 \pm 0.24	90.24 \pm 0.41	90.48 \pm 0.22	85.31 \pm 0.35	91.26 \pm 0.35	85.64 \pm 0.52	92.12 \pm 0.27	87.06 \pm 0.43
SDFed	98.27\pm0.12	93.54\pm0.25	91.05\pm0.11	87.12\pm0.18	94.72\pm0.21	89.45\pm0.32	94.68\pm0.15	90.04\pm0.25

**Figure 3: Convergence comparison between SDFed and baseline methods on single-domain datasets with 10 clients.**

Through choosing a diminishing step size $\beta = \Theta(1/\sqrt{ZO})$, Theorem 2 yields the typical non-convex rate $\min_{0 \leq z \leq Z-1} \mathbb{E} \|\nabla_{G_s} F(\cdot)\|_F^2 = \mathcal{O}\left(\frac{1}{\sqrt{ZO}}\right) + \mathcal{O}\left(\frac{O\delta^2}{ZO}\right)$, showing convergence to an ε -stationary point as ZO grows. The proof is in Appendix C.6.

3.6 Privacy Analysis

Our protocol does not introduce additional privacy leakage beyond standard FedAvg under the usual server model. In each round, the server observes only the uploaded global prompt $\{G_{s,l}^{z,O}\}_{l \in \mathcal{S}_z}$ and performs weighted averaging (Eq. (5)). All newly introduced components: client-specific local prompts $G_{c,l}$, the subspace projector $R^{z,o} = X_2 X_2^\top$, and the stretch or separate regularizers in Eq. (12)–(14) are computed locally and never transmitted. Therefore, the server-side transcript is isomorphic to FedAvg applied to the shared

parameter block G_s , implying any server-side inference or attack based on communications can be reduced to an attack on FedAvg with the same observables. Moreover, our method is orthogonal to existing privacy defenses: one can directly apply secure aggregation to the uploaded prompts, or enforce record-level or client-level differential privacy by clipping and perturbing the uploaded update $\Delta_{s,l}^z = G_{s,l}^{z,O} - G_s^{(z,0)}$ before Eq. (5). By DP post-processing invariance [2, 10], the local subspace refinement and regularizers do not weaken the resulting privacy guarantee.

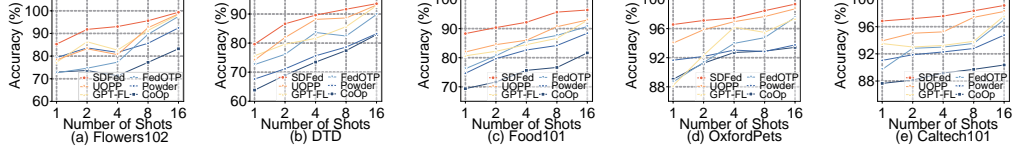


Figure 4: Test accuracy of SDFed on single domain datasets across different numbers of shots.

4 Experiments

4.1 Experimental Setup

Datasets. This study conducts a comprehensive evaluation on multiple public benchmark datasets with pronounced data heterogeneity. Five single-domain visual classification datasets are used: Flowers102 [31], DTD [6], Food101 [4], OxfordPets [33], and Caltech101 [11]. A pathological non-IID partitioning strategy assigns each client several non-overlapping classes to create heterogeneous distributions. Additionally, two multi-domain datasets, Office31 [36] and OfficeHome [42], are included, where each client accesses data from one domain, intensifying inter-client discrepancies. Moreover, experiments are conducted on two classical image benchmark datasets, CIFAR-10 [18] and Tiny-ImageNet [20]. In these datasets, data are randomly partitioned according to a symmetric Dirichlet distribution with the concentration parameter set to 0.3 following [12, 16, 38, 39].

Baselines. We compare SDFed with several popular state-of-the-art federated prompt learning methods, including CoOp [56], Powder [35], FedOTP [22], GPT-FL [55], and UOPP [29].

Evaluation Metrics. We evaluate each client on its private test set, drawn from the same distribution as its local training data, and report the mean test accuracy over all clients. For fair comparison, all methods use the same prompt length. Each experiment is repeated over five random seeds, we report the average, and all gains are statistically significant with $p\text{-value} < 0.05$.

Implementation Details. The experiments use hardware equipped with an AMD EPYC 7742 CPU, 512 GB of RAM, and an NVIDIA Tesla A100 GPU. All methods are evaluated on a frozen CLIP model with two backbone architectures, ViT B16 [9] and ResNet50 [15]. Each client performs 1 local training epoch, and the total number of federated communication rounds is 50. For the CIFAR-10 and Tiny ImageNet datasets, the number of communication rounds is adjusted to 25. The final performance is obtained by averaging the results of the last 10 rounds. The hyperparameters are set as $\lambda = 0.6$ and $\gamma = 0.8$. The model is trained using the SGD optimizer with a learning rate configured at 0.01. The learnable prompt length is 8, and the embedding dimension is 512. In heterogeneous environments, the local prompt length for each client varies between 4 to 64, while the global prompt length remains 8. The batch size is 16 for training and 64 for testing. For single-domain datasets, there are 10 clients, each with a distinct subset of classes. In multi-domain datasets, the number of clients is twice the number of domains, and each domain is divided equally among two clients. For CIFAR-10 and Tiny ImageNet, there are 100 clients, each randomly assigned 10% of the training data.

Table 4: Comparison under model heterogeneity.

Method	Flowers102	DTD	Food101	OxfordPets	Caltech101
CoOp	79.24 \pm 0.92	76.54 \pm 2.56	77.85 \pm 2.45	89.12 \pm 1.54	86.42 \pm 0.85
Powder	88.54 \pm 0.74	77.12 \pm 3.12	84.32 \pm 0.84	90.25 \pm 0.68	91.32 \pm 0.92
FedOTP	93.67 \pm 0.35	83.45 \pm 0.58	86.54 \pm 0.42	93.12 \pm 0.31	93.45 \pm 0.35
GPT-FL	95.21 \pm 0.52	87.56 \pm 0.64	89.42 \pm 0.48	94.56 \pm 0.55	94.12 \pm 0.62
UOPP	96.08 \pm 1.45	88.62 \pm 0.82	90.15 \pm 0.35	95.84 \pm 0.42	95.67 \pm 0.74
SDFed	97.56\pm0.21	90.34\pm0.35	93.42\pm0.22	97.68\pm0.18	97.24\pm0.31

Table 5: Runtime overhead of the Subspace Refinement for Local Prompts Method. Local model training is the total time of local model training.

Operational Phase	Time (ms)	Overhead
Global Prompt Decomposition	5.1	<1%
Local Prompt Projection	3.2	<1%
Global Prompt Aggregation	0.8	<1%
Local Model Training	4529.6	-

Table 6: Ablation study of SDFed performance after removing each component individually.

Module	Accuracy							
	PFHF	SPLP	IRDC	Flowers102	DTD	Food101	OxfordPets	Caltech101
✗	✗	✗	✗	91.27 \pm 0.78	86.51 \pm 1.45	87.63 \pm 0.82	91.05 \pm 0.94	91.22 \pm 1.15
✓	✗	✗	✗	93.64 \pm 0.52	88.06 \pm 1.12	90.07 \pm 0.58	94.74 \pm 0.64	93.98 \pm 0.82
✓	✓	✗	✗	95.89 \pm 0.34	89.96 \pm 0.85	92.35 \pm 0.42	96.13 \pm 0.41	96.80 \pm 0.56
✓	✗	✓	✗	96.88 \pm 0.25	91.82 \pm 0.54	94.31 \pm 0.31	96.97 \pm 0.32	98.26 \pm 0.38
✓	✓	✓	✗	99.35\pm0.07	93.56\pm0.18	96.38\pm0.06	99.36\pm0.07	99.12\pm0.11

4.2 Main Experiments

4.2.1 Single-Domain Analysis. To evaluate the applicability of SDFed with a fixed prompt length, we conduct experiments on single-domain datasets with pathological non-IID partitions. As shown in Tab. 1, the 16-shot results demonstrate that SDFed achieves the best accuracy across five datasets, outperforming the strongest baseline UOPP by up to 3.44% with lower variance. Unlike approaches that use a uniform prompt length, SDFed employs a globally fixed prompt together with client-specific variable-length local prompts, which enhances personalized representations and maintains strong performance on data with diverse styles. SDFed yields notable gains on Food101, which presents substantial inter- and intra-class variation, and on the fine-grained OxfordPets dataset, further demonstrating that explicitly modeling and constraining the global-to-local discrepancy in federated prompt learning effectively mitigates aggregation conflicts induced by heterogeneity.

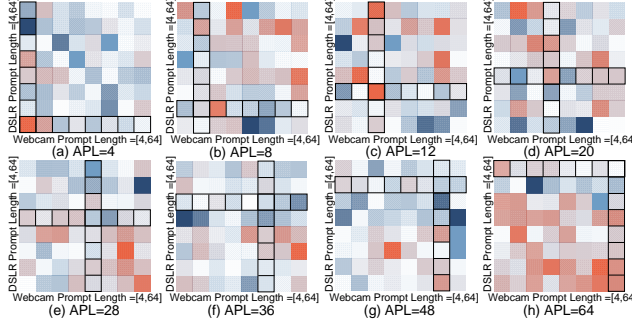


Figure 5: Effect of prompt length configurations on overall accuracy. Amazon Prompt Length is abbreviated as APL.

4.2.2 Multi-Domain Analysis. To model client heterogeneity, following [1, 16, 17], we use a Dirichlet distribution with concentration 0.3 to split each domain into two clients. SDFed is systematically evaluated on multi-domain datasets. Tab. 2 and Tab. 3 present both the overall average performance across all clients and the per-domain averages. On Office31 and OfficeHome, SDFed consistently outperforms the runner-up method across all domains. In contrast, UOPP fails to balance stylistic and semantic differences among domains, highlighting SDFed’s robustness under diverse domain settings.

4.2.3 Convergence Analysis. As shown in Fig. 3, we present the convergence curves over 50 training rounds. The figure indicates that SDFed rapidly reaches a stable regime within a few iterations, exhibiting faster convergence and higher final accuracy.

4.2.4 Model Heterogeneous Analysis. To evaluate robustness under system-level heterogeneity, we consider a model-heterogeneous federated setting with different backbones and computation budgets. The detailed experimental setup is shown in Appendix B. Tab. 4 reports overall average accuracy on five single-domain datasets, where SDFed consistently achieves the best performance, indicating robustness to backbone and budget heterogeneity.

4.2.5 Computational Overhead of Subspace Refinement. To quantify the computational overhead of Subspace Refinement for Local Prompts, we measured its client-side runtime cost, with averages reported over ten communication rounds in Tab. 5. The Subspace Refinement is executed only once per communication round, minimizing its impact. Relative to standard training, it occupies less than 1% of the total time, making it an almost negligible burden. Additionally, both global prompt decomposition and local prompt projection are low-rank updates performed locally, while the server only aggregates the global prompt, avoiding costly operations related to local prompts.

4.3 Ablation Study

We evaluate the effectiveness of three key components, namely the Prompt Driven Federated Heterogeneous Framework (PFHF), Subspace Refinement for Local Prompts (SRLP), and Information Retention and Divergence Control (IRDC), with the results shown in Tab. 6. Using PFHF alone improves accuracy on Flowers102

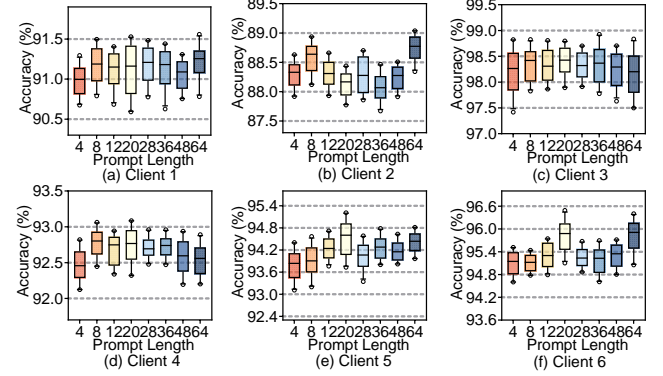


Figure 6: Effect of prompt length on client-side performance.

Table 7: Comparison of SDFed variants and baseline methods across 100 clients.

Method	CIFAR-10	Tiny-ImageNet
CoOp	89.76±0.12	47.78±0.21
Powder	92.68±0.16	53.69±0.07
FedOTP	92.95±0.14	53.13±0.11
GPT-FL	93.24±0.31	55.92±0.52
UOPP	94.32±0.39	56.19±0.41
SDFed ($S_l = 8$)	95.21±0.15	56.81±0.14
SDFed ($S_l \in [4, 64]$)	94.91±0.18	56.52±0.15

by 2.59%, indicating that aligning a globally shared fixed-length prompt with client-specific variable-length prompts enhances the balance between aggregation and personalization. Adding SRLP further improves performance across all datasets, as subspace refinement alleviates conflicts between local and global prompts and strengthens personalized representations. When both SRLP and IRDC are applied, accuracy on Flowers102 reaches 99.35%, demonstrating that this combination effectively reduces conflicts while maintaining information integrity.

4.4 Hyperparameter Analysis

4.4.1 Sensitivity Analysis. Fig. 4 illustrates the effect of varying the number of shots. Across all settings, SDFed consistently surpasses baseline methods. When the number of shots is small, baselines show a sharp accuracy drop, whereas SDFed maintains only a slight decrease compared with the 16-shot level. These findings indicate that SDFed offers stronger robustness and sample efficiency, enabling rapid adaptation to and characterization of client-specific requirements even under very low shot conditions.

4.4.2 Cross-domain Prompt Length Heterogeneity Analysis. We present in Fig. 5 how heterogeneous prompt lengths effect cross-domain performance on Office31. Candidate lengths for Amazon, Webcam, and DSLR are [4, 8, 12, 20, 28, 36, 48, 64]. Fixing Amazon’s length, we enumerate Webcam and DSLR combinations and report accuracy, with warm and cool colors denoting higher and lower performance, respectively. Black boxes mark combinations matching Amazon’s length. Most high-accuracy points lie outside these boxes, indicating that a uniform prompt length is suboptimal

and cannot meet the differentiated needs arising from data heterogeneity. By allowing client-specific prompt lengths, SDFed better adapts to cross-client distributional differences and maintains a performance advantage.

4.4.3 Intra Domain Prompt Length Heterogeneity Analysis. Fig. 6 shows how prompt length combinations affect client performance on Office31. Within each domain, paired clients share identical prompt length settings: clients 1 and 2, 3 and 4, and 5 and 6. The boxplot center line marks the median accuracy. Clients in the same domain display similar sensitivity to prompt length; for example, clients 5 and 6 peak at length 20 and dip at length 4. Sensitivity differs across domains: client 2 is optimal at length 64, whereas client 4 is optimal at length 20.

4.4.4 Robustness Analysis. To evaluate robustness under heterogeneity, we conduct a prompt length perturbation on CIFAR-10 and Tiny-ImageNet. All baselines use length 8. SDFed fixed assigns 8 tokens per client, whereas SDFed random samples a length from 4 to 64 per client. Tab. 7 shows SDFed yields the best overall accuracy and stronger cross-distribution generalization under non-IID settings. The fixed variant is slightly better than the random one because random lengths can mismatch client-specific distributions, causing local performance loss.

5 Conclusion

We introduce SDFed, a federated prompt learning framework designed to bridge global and local discrepancies in heterogeneous client environments. By adapting prompt lengths, SDFed enables efficient knowledge sharing while preserving personalization. The Subspace Refinement for Local Prompts Method removes conflicting representations and enhances local discriminability, while the Information Retention and Divergence Control Strategy maintains balanced alignment between shared and client-specific knowledge. Experiments demonstrate that SDFed outperforms existing methods and effectively addresses heterogeneity.

References

- [1] Xuming An, Li Shen, Han Hu, and Yong Luo. 2023. Federated learning with manifold regularization and normalized update reaggregation. *Advances in Neural Information Processing Systems* 36 (2023), 55097–55109.
- [2] Borja Balle and Yu-Xiang Wang. 2018. Improving the gaussian mechanism for differential privacy: Analytical calibration and optimal denoising. In *International conference on machine learning*. PMLR, 394–403.
- [3] Enrique Tomás Martínez Beltrán, Mario Quiles Pérez, Pedro Miguel Sánchez Sánchez, Sergio López Bernal, Gérôme Bovet, Manuel Gil Pérez, Gregorio Martínez Pérez, and Alberto Huertas Celdrán. 2023. Decentralized federated learning: Fundamentals, state of the art, frameworks, trends, and challenges. *IEEE Communications Surveys & Tutorials* 25, 4 (2023), 2983–3013.
- [4] Lukas Bossard, Matthieu Guillaumin, and Luc Van Gool. 2014. Food-101-mining discriminative components with random forests. In *European conference on computer vision*. Springer, 446–461.
- [5] Huancheng Chen and Haris Vikalo. 2024. Heterogeneity-guided client sampling: Towards fast and efficient non-IID federated learning. *Advances in Neural Information Processing Systems* 37 (2024), 65525–65561.
- [6] Mircea Cimpoi, Subhransu Maji, Iasonas Kokkinos, Sammy Mohamed, and Andrea Vedaldi. 2014. Describing textures in the wild. In *Proceedings of the IEEE conference on computer vision and pattern recognition*. 3606–3613.
- [7] Tianyu Cui, Hongxia Li, Jingya Wang, and Ye Shi. 2024. Harmonizing generalization and personalization in federated prompt learning. *arXiv preprint arXiv:2405.09771* (2024).
- [8] Xue Dong, Xuemeng Song, Tongliang Liu, and Weili Guan. 2025. Prompt-based multi-interest learning method for sequential recommendation. *IEEE Transactions on Pattern Analysis and Machine Intelligence* (2025).
- [9] Alexey Dosovitskiy. 2020. An image is worth 16x16 words: Transformers for image recognition at scale. *arXiv preprint arXiv:2010.11929* (2020).
- [10] Cynthia Dwork, Aaron Roth, et al. 2014. The algorithmic foundations of differential privacy. *Foundations and trends® in theoretical computer science* 9, 3–4 (2014), 211–407.
- [11] Li Fei-Fei, Rob Fergus, and Pietro Perona. 2004. Learning generative visual models from few training examples: An incremental bayesian approach tested on 101 object categories. In *2004 conference on computer vision and pattern recognition workshop*. IEEE, 178–178.
- [12] Liang Gao, Huazhu Fu, Li Li, Yingwen Chen, Ming Xu, and Cheng-Zhong Xu. 2022. Feddc: Federated learning with non-iid data via local drift decoupling and correction. In *Proceedings of the IEEE/CVF conference on computer vision and pattern recognition*. 10112–10121.
- [13] Tao Guo, Song Guo, and Junxiao Wang. 2023. Pfedprompt: Learning personalized prompt for vision-language models in federated learning. In *Proceedings of the ACM Web Conference 2023*. 1364–1374.
- [14] Tao Guo, Song Guo, Junxiao Wang, Xueyang Tang, and Wenchao Xu. 2023. Promptptf: Let federated participants cooperatively learn prompts instead of models–federated learning in age of foundation model. *IEEE Transactions on Mobile Computing* 23, 5 (2023), 5179–5194.
- [15] Kaiming He, Xiangyu Zhang, Shaoqing Ren, and Jian Sun. 2016. Deep residual learning for image recognition. In *Proceedings of the IEEE conference on computer vision and pattern recognition*. 770–778.
- [16] Geoho Kim, Jinkyu Kim, and Bohyung Han. 2024. Communication-efficient federated learning with accelerated client gradient. In *Proceedings of the IEEE/CVF Conference on Computer Vision and Pattern Recognition*. 12385–12394.
- [17] Jinkyu Kim, Geoho Kim, and Bohyung Han. 2022. Multi-level branched regularization for federated learning. In *International Conference on Machine Learning*. PMLR, 11058–11073.
- [18] Alex Krizhevsky, Geoffrey Hinton, et al. 2009. Learning multiple layers of features from tiny images. (2009).
- [19] Fan Lai, Yinwei Dai, Sanjay Singapuram, Jiachen Liu, Xiangfeng Zhu, Harsha Madhyastha, and Mosharaf Chowdhury. 2022. Fedscale: Benchmarking model and system performance of federated learning at scale. In *International conference on machine learning*. PMLR, 11814–11827.
- [20] Yann Le and Xuan Yang. 2015. Tiny imagenet visual recognition challenge. *CS 231N* 7, 7 (2015), 3.
- [21] Hongxia Li, Wei Huang, Jingya Wang, and Ye Shi. 2024. Global and local prompts cooperation via optimal transport for federated learning. In *Proceedings of the IEEE/CVF Conference on Computer Vision and Pattern Recognition*. 12151–12161.
- [22] Hongxia Li, Wei Huang, Jingya Wang, and Ye Shi. 2024. Global and local prompts cooperation via optimal transport for federated learning. In *Proceedings of the IEEE/CVF Conference on Computer Vision and Pattern Recognition*. 12151–12161.
- [23] Qinbin Li, Bingsheng He, and Dawn Song. 2021. Model-contrastive federated learning. In *Proceedings of the IEEE/CVF conference on computer vision and pattern recognition*. 10713–10722.
- [24] Zhengpin Li, Minhua Lin, Jian Wang, and Suhang Wang. 2025. Fairness-aware prompt tuning for graph neural networks. In *Proceedings of the ACM on Web Conference 2025*. 3586–3597.
- [25] Jianchun Liu, Jiameng Yan, Hongli Xu, Lun Wang, Zhiyuan Wang, Jinyang Huang, and Chunming Qiao. 2025. Accelerating decentralized federated learning with probabilistic communication in heterogeneous edge computing. *IEEE Transactions on Networking* (2025).
- [26] Jiahao Liu, Yipeng Zhou, Di Wu, Miao Hu, Mohsen Guizani, and Quan Z. Sheng. 2024. FedLMT: tackling system heterogeneity of federated learning via low-rank model training with theoretical guarantees. In *Proceedings of the 41st International Conference on Machine Learning*. Article 1319, 43 pages.
- [27] Yang Liu, Yan Kang, Tianyuan Zou, Yanhong Pu, Yuanqin He, Xiaozhou Ye, Ye Ouyang, Ya-Qin Zhang, and Qiang Yang. 2024. Vertical federated learning: Concepts, advances, and challenges. *IEEE transactions on knowledge and data engineering* 36, 7 (2024), 3615–3634.
- [28] Sifan Long, Zhen Zhao, Junkun Yuan, Zichang Tan, Jiangjiang Liu, Jingyuany Feng, Shengsheng Wang, and Jingdong Wang. 2025. Mutual prompt leaning for vision language models. *International Journal of Computer Vision* 133, 3 (2025), 1258–1276.
- [29] Muhammad Anwar Ma’sum, Mahardhika Pratama, Lin Liu, Habibullah Habibullah, and Ryszard Kowalczyk. 2025. Federated Few-Shot Class-Incremental Learning. In *The Thirteenth International Conference on Learning Representations*.
- [30] Brendan McMahan, Eider Moore, Daniel Ramage, Seth Hampson, and Blaise Agüera y Arcas. 2017. Communication-efficient learning of deep networks from decentralized data. In *Artificial intelligence and statistics*. PMLR, 1273–1282.
- [31] Maria-Elena Nilsback and Andrew Zisserman. 2008. Automated flower classification over a large number of classes. In *2008 Sixth Indian conference on computer vision, graphics & image processing*. IEEE, 722–729.
- [32] Bikang Pan, Wei Huang, and Ye Shi. 2024. Federated learning from vision-language foundation models: Theoretical analysis and method. *Advances in Neural Information Processing Systems* 37 (2024), 30590–30623.

[33] Omkar M Parkhi, Andrea Vedaldi, Andrew Zisserman, and CV Jawahar. 2012. Cats and dogs. In *2012 IEEE conference on computer vision and pattern recognition*. IEEE, 3498–3505.

[34] Jiaming Pei, Wenxuan Liu, Jinhai Li, Lukun Wang, and Chao Liu. 2024. A review of federated learning methods in heterogeneous scenarios. *IEEE Transactions on Consumer Electronics* 70, 3 (2024), 5983–5999.

[35] Hongming Piao, Yichen Wu, Dapeng Wu, and Ying Wei. 2024. Federated continual learning via prompt-based dual knowledge transfer. In *Forty-first International Conference on Machine Learning*.

[36] Kate Saenko, Brian Kulis, Mario Fritz, and Trevor Darrell. 2010. Adapting visual category models to new domains. In *European conference on computer vision*. Springer, 213–226.

[37] Jiangming Shi, Shanshan Zheng, Xiangbo Yin, Yang Lu, Yuan Xie, and Yanyan Qu. 2024. Clip-guided federated learning on heterogeneity and long-tailed data. In *Proceedings of the AAAI Conference on Artificial Intelligence*, Vol. 38. 14955–14963.

[38] Yifan Shi, Yingqi Liu, Kang Wei, Li Shen, Xueqian Wang, and Dacheng Tao. 2023. Make landscape flatter in differentially private federated learning. In *Proceedings of the IEEE/CVF conference on computer vision and pattern recognition*. 24552–24562.

[39] Yifan Shi, Li Shen, Kang Wei, Yan Sun, Bo Yuan, Xueqian Wang, and Dacheng Tao. 2023. Improving the model consistency of decentralized federated learning. In *International conference on machine learning*. PMLR, 31269–31291.

[40] Qi Tan, Yi Zhao, Qi Li, and Ke Xu. 2025. Expediting Federated Learning on Non-IID Data by Maximizing Communication Channel Utilization. *IEEE Transactions on Networking* (2025).

[41] Linh Tran, Wei Sun, Stacy Patterson, and Ana Milanova. 2025. Privacy-preserving personalized federated prompt learning for multimodal large language models. *arXiv preprint arXiv:2501.13904* (2025).

[42] Hemant Venkateswara, Jose Eusebio, Shayok Chakraborty, and Sethuraman Panchanathan. 2017. Deep hashing network for unsupervised domain adaptation. In *Proceedings of the IEEE conference on computer vision and pattern recognition*. 5018–5027.

[43] Jianyu Wang, Qinghua Liu, Hao Liang, Gauri Joshi, and H Vincent Poor. 2020. Tackling the objective inconsistency problem in heterogeneous federated optimization. *Advances in neural information processing systems* 33 (2020), 7611–7623.

[44] Fu-En Yang, Chien-Yi Wang, and Yu-Chiang Frank Wang. 2023. Efficient model personalization in federated learning via client-specific prompt generation. In *Proceedings of the IEEE/CVF International Conference on Computer Vision*. 19159–19168.

[45] Mang Ye, Wei Shen, Bo Du, Eduard Snelzhko, Vassili Kovalev, and Pong C Yuen. 2025. Vertical federated learning for effectiveness, security, applicability: A survey. *Comput. Surveys* 57, 9 (2025), 1–32.

[46] Liping Yi, Gang Wang, Xiaoguang Liu, Zhan Shi, and Han Yu. 2023. Fedgh: Heterogeneous federated learning with generalized global header. In *Proceedings of the 31st ACM international conference on multimedia*. 8686–8696.

[47] Hao Yu, Xin Yang, Le Zhang, Hanlin Gu, Tianrui Li, Lixin Fan, and Qiang Yang. 2025. Handling spatial-temporal data heterogeneity for federated continual learning via tail anchor. In *Proceedings of the Computer Vision and Pattern Recognition Conference*. 4874–4883.

[48] Wentao Yu, Shuo Chen, Yongxin Tong, Tianlong Gu, and Chen Gong. 2025. Modeling inter-intra heterogeneity for graph federated learning. In *Proceedings of the AAAI Conference on Artificial Intelligence*, Vol. 39. 22236–22244.

[49] Lixiang Yuan, Jiapeng Zhang, Mingxing Duan, Guoqing Xiao, Zhuo Tang, and Kenli Li. 2025. PRFL: Personalized and Robust Federated Learning for Non-IID Data with Malicious Participants. *IEEE Transactions on Mobile Computing* (2025).

[50] Wei Yuan, Liang Qu, Lizhen Cui, Yongxin Tong, Xiaofang Zhou, and Hongzhi Yin. 2024. Hetefedrec: Federated recommender systems with model heterogeneity. In *2024 IEEE 40th International Conference on Data Engineering (ICDE)*. IEEE, 1324–1337.

[51] Jianqing Zhang, Yang Liu, Yang Hua, Hao Wang, Tao Song, Zhengui Xue, Ruhui Ma, and Jian Cao. 2025. Pfllib: A beginner-friendly and comprehensive personalized federated learning library and benchmark. *Journal of Machine Learning Research* 26, 50 (2025), 1–10.

[52] Jianqing Zhang, Xinghao Wu, Yanbing Zhou, Xiaoting Sun, Qiqi Cai, Yang Liu, Yang Hua, Zhenzhe Zheng, Jian Cao, and Qiang Yang. 2025. Htllib: A comprehensive heterogeneous federated learning library and benchmark. In *Proceedings of the 31st ACM SIGKDD Conference on Knowledge Discovery and Data Mining* V. 2. 5900–5911.

[53] Junyuan Zhang, Shuang Zeng, Miao Zhang, Runxi Wang, Feifei Wang, Yuyin Zhou, Paul Pu Liang, and Liangqiong Qu. 2024. Flhेत्वेन्चेन: Benchmarking device and state heterogeneity in federated learning. In *Proceedings of the IEEE/CVF Conference on Computer Vision and Pattern Recognition*. 12098–12108.

[54] Tuo Zhang, Tiantian Feng, Samiul Alam, Dimitrios Dimitriadis, Sunwoo Lee, Mi Zhang, Shrikanth S Narayanan, and Salman Avestimehr. 2025. Gpt-fl: Generative pre-trained model-assisted federated learning. In *Proceedings of the Computer Vision and Pattern Recognition Conference*. 1761–1770.

[55] Tuo Zhang, Tiantian Feng, Samiul Alam, Dimitrios Dimitriadis, Sunwoo Lee, Mi Zhang, Shrikanth S Narayanan, and Salman Avestimehr. 2025. Gpt-fl: Generative

Table 8: Notation list.

Symbol	Description
M, I	the number of clients and client index
Ω_I, h_I	the client- I dataset and dataset size
w_I	the aggregation weight
B, z	the communication rounds and round index
\mathbb{S}_z	the selected clients in round z
O, o	the local steps and step index
m	the CLIP embedding dimension
K_{\max}	the maximum input token length
$V = \{v_1, \dots, v_c\}$	the fixed class word embeddings
e_{st}, e_{en}	the trainable start token and trainable end token
e_{la}, e_{su}, e_{pa}	the label token and suffix token and padding token
G_e	the learnable context vectors
$G_s^{(z,0)}$	the global prompt at round start
$G_s^{z,0}$	the client- I global prompt after local training
$G_{s,l}^{z,o}$	the client- I local prompt at step o
$s(\cdot), \hat{s}_g$	the CLIP text encoder and prompt-aware text feature
$d(\cdot), d$	the frozen encoder and image feature
$\text{sim}(\cdot, \cdot), \mu$	the cosine similarity and temperature
$\mathcal{L}_{ce}, \mathcal{L}$	the cross-entropy loss and total loss
β, γ	the learning rate and separation margin
$G_s^{z,o} = HZX^\top$	the SVD of the global prompt
H, Z, X	the left singular vectors and singular values and right singular vectors
λ, r, m'	the truncation ratio and $r = \lfloor \lambda m \rfloor$ and $m' = m - r$
$X_2, R^{z,o}$	the truncated right subspace and projection matrix
$\tilde{G}_{s,l}^{z,o}$	the refined local prompt
$\mathcal{L}_{str}, \mathcal{L}_{sep}$	the stretch loss and separation loss

pre-trained model-assisted federated learning. In *Proceedings of the Computer Vision and Pattern Recognition Conference*. 1761–1770.

[56] Kaiyang Zhou, Jingkang Yang, Chen Change Loy, and Ziwei Liu. 2022. Learning to prompt for vision-language models. *International Journal of Computer Vision* 130, 9 (2022), 2337–2348.

[57] Jiawen Zhu, Simiao Lai, Xin Chen, Dong Wang, and Huchuan Lu. 2023. Visual prompt multi-modal tracking. In *Proceedings of the IEEE/CVF conference on computer vision and pattern recognition*. 9516–9526.

A Notation

We summarize the key notations used throughout the paper. For clarity, we list the main variables, operators, and hyperparameters in Tab. 8.

B Model Heterogeneity Client Configuration

We describe the client configuration used to evaluate robustness under system-level model heterogeneity in federated learning. To capture the diverse system capabilities in real-world cross-device scenarios, we adopt a model-heterogeneous setting with different backbones and computation budgets across clients. Following prior work [19, 53], we use a 2-3-5 split to simulate the skewed distribution of device resources:

- **Strong clients:** Assigned a higher computation budget with larger batch sizes and more local epochs, using the computationally demanding ViT-B16 backbone.
- **Medium clients:** Have a medium computation budget and also use ViT-B16, but with fewer resources.
- **Weak clients:** Resource-constrained clients with a small batch size and step cap, using the less expensive ResNet50 backbone, representing the majority of clients.

Tab. 9 summarizes each client type’s configuration. This heterogeneous setup reflects a diverse federated learning environment, with clients of varying capabilities contributing to model training.

Table 9: Client configuration under model heterogeneity.

Client Type	#Clients	Backbone	Batch	Local Epoch	Step Cap
Strong	2	ViT-B16	32	2	–
Medium	3	ViT-B16	16	1	–
Weak	5	ResNet50	8	1	50

C Proofs

C.1 Proof of Lemma 1

PROOF. Let $G_s^{z,o} = HZX^\top$ with $X = [x_1, \dots, x_m]$ orthogonal and singular values sorted. Set $r = \lfloor \lambda m \rfloor$, $X_2 = [x_{r+1}, \dots, x_m] \in \mathcal{R}^{m \times m'}$ ($m' = m - r$), and $R^{z,o} = X_2 X_2^\top$. Since $X_2^\top X_2 = I$, we have:

$$(R^{z,o})^\top = R^{z,o}, (R^{z,o})^2 = X_2 (X_2^\top X_2) X_2^\top = R^{z,o}, \quad (21)$$

so $R^{z,o}$ is the orthogonal projector onto $\text{span}(X_2)$.

For any row vector $u \in \mathcal{R}^{1 \times m}$, expand in the basis $\{x_i\}_{i=1}^m$: $u = \sum_{i=1}^m \alpha_i x_i^\top$ with $\alpha_i = ux_i$. Then, we have:

$$u R^{z,o} = u X_2 X_2^\top = \sum_{i=r+1}^m \alpha_i x_i^\top, u(I - R^{z,o}) = \sum_{i=1}^r \alpha_i x_i^\top. \quad (22)$$

Hence right-multiplication by $R^{z,o}$ removes the components along $\{x_1, \dots, x_r\}$ and retains those along $\{x_{r+1}, \dots, x_m\}$. Applying this row-wise to $G_{c,l}^{z,o}$ gives $\tilde{G}_{c,l}^{z,o} = G_{c,l}^{z,o} R^{z,o}$. \square

C.2 Proof of Lemma 2

PROOF. Fix any (z, o) and write $R := R^{z,o}$. By Assumption 4, R is a symmetric idempotent projector and $\|R\|_2 \leq 1$. For any $A \in \mathcal{R}^{S_l \times m}$, by submultiplicativity of the Frobenius norm, we have:

$$\|AR\|_F \leq \|A\|_F \|R\|_2 \leq \|A\|_F. \quad (23)$$

Moreover, we have

$$\|A - AR\|_F = \|A(I - R)\|_F \leq \|A\|_F \|I - R\|_2. \quad (24)$$

Since R is an orthogonal projector, its eigenvalues lie in $\{0, 1\}$, hence $\|I - R\|_2 \leq 1$. Therefore $\|A - AR\|_F \leq \|A\|_F$. \square

C.3 Proof of Lemma 3

PROOF. Let $f_l = f_{ce,l} + \mathcal{L}_{str,l} + \mathcal{L}_{sep,l}$. By Assumption 1, $f_{ce,l}$ is L -smooth. Fix (z, o) and denote $R := R^{z,o}$. Since R is an orthogonal projector with $\|R\|_2 \leq 1$ (Assumption 4), the map $T(G) = GR$ is non-expansive in Frobenius norm: $\|T(U) - T(V)\|_F \leq \|U - V\|_F$. Because $d(\cdot)$ is a fixed encoder, it is continuously differentiable and has Lipschitz Jacobian on any bounded set containing the prompt iterates; hence both $G \mapsto d(G)$ and $G \mapsto d(GR)$ have Lipschitz gradients. Therefore $G \mapsto d(G) - d(GR)$ has Lipschitz gradient, and $\mathcal{L}_{str}(G) = \|d(G) - d(GR)\|_F^2$ is smooth with some constant $L_{str} < \infty$. For $\mathcal{L}_{sep} = \text{ReLU}(\gamma - \|d(G_{c,l}) - d(G_s)\|_2)$, it is smooth everywhere except on the measure-zero boundary $\|d(G_{c,l}) - d(G_s)\|_2 = \gamma$, and admits bounded subgradients. Hence it does not affect the smoothness analysis.

Combining the above, f_l is L' -smooth almost everywhere with $L' = L + L_{str} = \Theta(L)$, and admits bounded subgradients everywhere. \square

C.4 Proof of Lemma 4

PROOF. Let $G := G_{c,l}^{z,o}$ and $\tilde{G} := \tilde{G}_{c,l}^{z,o}$. With $\mathcal{L}_{str} = \|d(G) - d(\tilde{G})\|_2^2$, treating \tilde{G} as fixed in this term gives:

$$\nabla_G \mathcal{L}_{str} = 2 J_d(G)^\top (d(G) - d(\tilde{G})). \quad (25)$$

Since d is L_d -Lipschitz, it is a.e. differentiable with $\|J_d(G)\|_2 \leq L_d$, hence we have:

$$\begin{aligned} \|\nabla_G \mathcal{L}_{str}\|_F &\leq 2 \|J_d(G)\|_2 \|d(G) - d(\tilde{G})\|_2 \\ &\leq 2 L_d \|d(G) - d(\tilde{G})\|_2 \\ &\leq 2 L_d^2 \|G - \tilde{G}\|_F. \end{aligned} \quad (26)$$

Let $\Delta := d(G_{c,l}^{z,o}) - d(\tilde{G}_{c,l}^{z,o})$ and $\mathcal{L}_{sep} = \text{ReLU}(\gamma - \|\Delta\|_2)$. If $\mathcal{L}_{sep} = 0$, take $g = 0$. If $\mathcal{L}_{sep} > 0$, a subgradient w.r.t. $G_{c,l}$ is:

$$g = -J_d(G_{c,l}^{z,o})^\top \frac{\Delta}{\|\Delta\|_2}, \quad (27)$$

thus we have:

$$\|g\|_F \leq \|J_d(G_{c,l}^{z,o})\|_2 \left\| \frac{\Delta}{\|\Delta\|_2} \right\|_2 \leq L_d. \quad (28)$$

\square

C.5 Proof of Theorem 1

PROOF. Fix (z, o) and client l . Denote $G := G_{c,l}^{z,o} \in \mathcal{R}^{S_l \times m}$ and $G_s := G_s^{z,o} \in \mathcal{R}^{S_s \times m}$. From the SVD (Eq. (8)), we have:

$$G_s = HZX^\top, \quad (29)$$

the columns $X = [x_1, \dots, x_m] \in \mathcal{R}^{m \times m}$ are orthonormal right-singular vectors with $\sigma_1 \geq \dots \geq \sigma_m \geq 0$. Let $\lambda \in (0, 1)$, $m' = \lfloor (1 - \lambda)m \rfloor$, and

$$X_2 := [x_{\lfloor \lambda m \rfloor + 1}, \dots, x_m] \in \mathcal{R}^{m \times m'}. \quad (30)$$

Define the refinement matrix (Eq. (10)), we have:

$$R := R^{z,o} = X_2 X_2^\top \in \mathcal{R}^{m \times m'} \mathcal{R}^{m' \times m} = \mathcal{R}^{m \times m}. \quad (31)$$

Since $X_2^\top X_2 = I_{m'}$, we have:

$$R^\top = R, R^2 = X_2 (X_2^\top X_2) X_2^\top = R, \quad (32)$$

so R is the orthogonal projector onto $\text{span}(X_2)$, and we set:

$$\tilde{G} := \tilde{G}_{c,l}^{z,o} = GR. \quad (33)$$

Step 1: Constraint set. Consider

$$\mathcal{S} := \{U \in \mathcal{R}^{S_l \times m} : U = UR\}. \quad (34)$$

For any row vector $u^\top \in \mathcal{R}^{1 \times m}$, $u^\top R$ is the Euclidean projection onto $\text{span}(X_2)$. Hence, we have:

$$U \in \mathcal{S} \iff \text{row}(U) \subseteq \text{span}(X_2). \quad (35)$$

Step 2: Frobenius-orthogonal decomposition. With $\langle A, B \rangle_F := \text{tr}(A^\top B)$, decompose

$$G = GR + G(I - R). \quad (36)$$

We have $GR \in \mathcal{S}$ since $(GR)R = GR^2 = GR$. For any $U \in \mathcal{S}$, also $U - GR \in \mathcal{S}$, so its rows lie in $\text{span}(X_2)$, whereas rows of $G(I - R)$ lie in $\text{span}(X_2)^\perp$. Thus, we have:

$$\langle U - GR, G(I - R) \rangle_F = 0. \quad (37)$$

Step 3: Optimality and uniqueness. For any feasible $U \in \mathcal{S}$, we have:

$$\begin{aligned} \|U - G\|_F^2 &= \|U - (GR + G(I - R))\|_F^2 \\ &= \|(U - GR) - G(I - R)\|_F^2 \\ &= \|U - GR\|_F^2 + \|G(I - R)\|_F^2 \geq \|G(I - R)\|_F^2, \end{aligned} \quad (38)$$

with equality iff $U = GR$. Therefore GR is the unique minimizer of

$$\min_{U \in \mathcal{R}^{S_l \times m}} \|U - G\|_F^2 \quad \text{s.t.} \quad U = UR, \quad (39)$$

and hence we have:

$$\tilde{G}_{c,l}^{z,o} = GR = G_{c,l}^{z,o} R^{z,o}. \quad (40)$$

□

C.6 Proof of Theorem 2

PROOF. Recall the global objective:

$$F(G_s, \{G_{c,l}\}_{l=1}^M) = \sum_{l=1}^M w_l f_l(G_s, G_{c,l}), \quad w_l = \frac{h_l}{\sum_{k=1}^M h_k}. \quad (41)$$

For clarity of constants, we present the proof under full participation and uniform aggregation. The weighted case follows by replacing $1/M$ with $\sum_{l=1}^M w_l^2$ in the variance term. Define the round-begin state:

$$\theta^{z,0} := \left(G_s^{(z,0)}, \{G_{c,l}^{z,0}\}_{l=1}^M \right), \quad F_z := F(\theta^{z,0}), \quad \nabla_s F_z := \nabla_{G_s} F(\theta^{z,0}). \quad (42)$$

At round z , client l initializes $G_{s,l}^{z,0} = G_s^{(z,0)}$ and performs O local SGD steps with stepsize β . Let $g_{s,l}^{z,o}$ be the stochastic gradient of f_l w.r.t. G_s at local step o . Telescoping the local updates yields:

$$G_{s,l}^{z,O} = G_s^{(z,0)} - \beta \sum_{o=0}^{O-1} g_{s,l}^{z,o}. \quad (43)$$

Under full participation and uniform aggregation, we have:

$$G_s^{(z+1,0)} = \frac{1}{M} \sum_{l=1}^M G_{s,l}^{z,O} = G_s^{(z,0)} - \beta \sum_{o=0}^{O-1} \left(\frac{1}{M} \sum_{l=1}^M g_{s,l}^{z,o} \right). \quad (44)$$

Define the round-averaged gradient estimator and effective stepsize, we have:

$$\hat{g}_z := \frac{1}{MO} \sum_{l=1}^M \sum_{o=0}^{O-1} g_{s,l}^{z,o}, \quad \eta := \beta O, \quad (45)$$

Then the server update is

$$G_s^{(z+1,0)} = G_s^{(z,0)} - \eta \hat{g}_z. \quad (46)$$

Let \mathcal{F}_z be the sigma-field generated by all randomness up to the beginning of round z . By Assumption 2,

$$\mathbb{E}[\hat{g}_z | \mathcal{F}_z] = \frac{1}{MO} \sum_{l=1}^M \sum_{o=0}^{O-1} \nabla_{G_s} f_l(G_{s,l}^{z,o}, G_{c,l}^{z,o}). \quad (47)$$

Define the bias term

$$b_z := \mathbb{E}[\hat{g}_z | \mathcal{F}_z] - \nabla_s F_z, \quad (48)$$

and the zero-mean noise

$$\xi_z := \hat{g}_z - \mathbb{E}[\hat{g}_z | \mathcal{F}_z], \quad \mathbb{E}[\xi_z | \mathcal{F}_z] = 0. \quad (49)$$

Then we have:

$$\hat{g}_z = \nabla_s F_z + b_z + \xi_z. \quad (50)$$

Let $g_{s,l}^{z,o} = \nabla_{G_s} f_l(\cdot) + \varepsilon_{l,o}$ where $\mathbb{E}[\varepsilon_{l,o} | \mathcal{F}_z] = 0$ and $\mathbb{E}\|\varepsilon_{l,o}\|_F^2 \leq \sigma^2$. We have:

$$\xi_z = \frac{1}{MO} \sum_{l,o} \varepsilon_{l,o}. \quad (51)$$

Using Jensen's inequality and bounded variance, we have:

$$\mathbb{E}\|\xi_z\|_F^2 \leq \frac{1}{M^2 O^2} \sum_{l,o} \mathbb{E}\|\varepsilon_{l,o}\|_F^2 \leq \frac{MO \cdot \sigma^2}{M^2 O^2} = \frac{\sigma^2}{MO}. \quad (52)$$

By definition,

$$b_z = \frac{1}{MO} \sum_{l,o} \nabla_{G_s} f_l(G_{s,l}^{z,o}, G_{c,l}^{z,o}) - \frac{1}{M} \sum_l \nabla_{G_s} f_l(G_s^{(z,0)}, G_{c,l}^{z,o}). \quad (53)$$

Add and subtract $\nabla_{G_s} f_l(G_s^{(z,0)}, G_{c,l}^{z,o})$ and apply triangle inequality:

$$\begin{aligned} \|b_z\|_F &\leq \left\| \frac{1}{MO} \sum_{l,o} \left(\nabla_{G_s} f_l(G_{s,l}^{z,o}, G_{c,l}^{z,o}) - \nabla_{G_s} f_l(G_s^{(z,0)}, G_{c,l}^{z,o}) \right) \right\|_F \\ &\quad + \left\| \frac{1}{MO} \sum_{l,o} \left(\nabla_{G_s} f_l(G_s^{(z,0)}, G_{c,l}^{z,o}) - \nabla_{G_s} f_l(G_s^{(z,0)}, G_{c,l}^{z,0}) \right) \right\|_F. \end{aligned} \quad (54)$$

By L' -smoothness in each argument, both terms are bounded by the average local drift. Under the stepsize condition $\beta \leq 1/(4L'O)$ and the heterogeneity envelope in Assumption 3, a standard Local-SGD drift bound gives:

$$\frac{1}{MO} \sum_{l,o} \mathbb{E}\|G_{s,l}^{z,o} - G_s^{(z,0)}\|_F \leq \eta \delta, \quad \frac{1}{MO} \sum_{l,o} \mathbb{E}\|G_{c,l}^{z,o} - G_{c,l}^{z,0}\|_F \leq \eta \delta, \quad (55)$$

hence $\mathbb{E}\|b_z\|_F \leq 2L' \eta \delta$ and therefore $\|b_z\|_F^2 \leq 4L'^2 \eta^2 \delta^2$. Since Lemma 3 implies F is L' -smooth in G_s , we have the descent lemma:

$$\begin{aligned} F(G_s^{(z+1,0)}, \{G_{c,l}^{z,0}\}) &\leq F_z + \left\langle \nabla_s F_z, G_s^{(z+1,0)} - G_s^{(z,0)} \right\rangle \\ &\quad + \frac{L'}{2} \|G_s^{(z+1,0)} - G_s^{(z,0)}\|_F^2. \end{aligned} \quad (56)$$

Plugging the update $G_s^{(z+1,0)} - G_s^{(z,0)} = -\eta \hat{g}_z$ from (46) and taking conditional expectation w.r.t. \mathcal{F}_z , using (50), yields:

$$\mathbb{E}[F_{z+1} | \mathcal{F}_z] \leq F_z - \eta \langle \nabla_s F_z, \nabla_s F_z + b_z \rangle + \frac{L' \eta^2}{2} \mathbb{E}\|\nabla_s F_z + b_z + \xi_z\|_F^2. \quad (57)$$

We upper bound the last two terms. First, by Young's inequality $-\langle a, b \rangle \leq \frac{1}{2}\|a\|^2 + \frac{1}{2}\|b\|^2$, we have:

$$-\eta \langle \nabla_s F_z, b_z \rangle \leq \frac{\eta}{2} \|\nabla_s F_z\|_F^2 + \frac{\eta}{2} \|b_z\|_F^2. \quad (58)$$

Second, using $\|a+b+c\|^2 \leq 2\|a+b\|^2 + 2\|c\|^2 \leq 4\|a\|^2 + 4\|b\|^2 + 2\|c\|^2$, we have:

$$\mathbb{E}\|\nabla_s F_z + b_z + \xi_z\|_F^2 \leq 4\|\nabla_s F_z\|_F^2 + 4\|b_z\|_F^2 + 2\mathbb{E}\|\xi_z\|_F^2. \quad (59)$$

Substituting (58)–(59) into (57) gives:

$$\begin{aligned} \mathbb{E}[F_{z+1} \mid \mathcal{F}_z] &\leq F_z - \eta \|\nabla_s F_z\|_F^2 + \frac{\eta}{2} \|V_s F_z\|_F^2 + \frac{\eta}{2} \|b_z\|_F^2 \\ &\quad + \frac{L' \eta^2}{2} (4 \|\nabla_s F_z\|_F^2 + 4 \|b_z\|_F^2 + 2 \mathbb{E}\|\xi_z\|_F^2) \\ &= F_z - \left(\frac{\eta}{2} - 2L' \eta^2\right) \|\nabla_s F_z\|_F^2 + \left(\frac{\eta}{2} + 2L' \eta^2\right) \|b_z\|_F^2 \\ &\quad + L' \eta^2 \mathbb{E}\|\xi_z\|_F^2. \end{aligned} \quad (60)$$

Under the stepsize condition $\eta = \beta O \leq \frac{1}{4L'}$, we have $\frac{\eta}{2} - 2L' \eta^2 \geq \frac{\eta}{4}$ and $\frac{\eta}{2} + 2L' \eta^2 \leq \eta$. Therefore, we have:

$$\mathbb{E}[F_{z+1} \mid \mathcal{F}_z] \leq F_z - \frac{\eta}{4} \|\nabla_s F_z\|_F^2 + \eta \|b_z\|_F^2 + L' \eta^2 \mathbb{E}\|\xi_z\|_F^2. \quad (61)$$

Taking full expectation and applying Eq. (52) with Eq. (55) yields:

$$\mathbb{E}[F_{z+1}] \leq \mathbb{E}[F_z] - \frac{\eta}{4} \mathbb{E}\|\nabla_s F_z\|_F^2 + 4L'^2 \eta^3 \delta^2 + \frac{L' \eta^2 \sigma^2}{MO}. \quad (62)$$

Summing Eq. (62) over $z = 0, \dots, Z-1$ and using $F_\star = \inf F$ gives:

$$\begin{aligned} \frac{\eta}{4} \sum_{z=0}^{Z-1} \mathbb{E}\|\nabla_s F_z\|_F^2 &\leq \mathbb{E}[F_0] - \mathbb{E}[F_Z] + 4L'^2 \eta^3 Z \delta^2 + \frac{L' \eta^2 Z \sigma^2}{MO} \\ &\leq (F_0 - F_\star) + 4L'^2 \eta^3 Z \delta^2 + \frac{L' \eta^2 Z \sigma^2}{MO}. \end{aligned} \quad (63)$$

Dividing by $\eta Z/4$ yields:

$$\frac{1}{Z} \sum_{z=0}^{Z-1} \mathbb{E}\|\nabla_s F_z\|_F^2 \leq \frac{4(F_0 - F_\star)}{\eta Z} + 16L'^2 \eta^2 \delta^2 + \frac{4L' \eta \sigma^2}{MO}. \quad (64)$$

Finally substitute $\eta = \beta O$, we have:

$$\begin{aligned} \frac{1}{Z} \sum_{z=0}^{Z-1} \mathbb{E}\|\nabla_{G_s} F(G_s^{(z,0)}, \{G_{c,l}^{z,0}\})\|_F^2 &\leq \frac{4(F_0 - F_\star)}{\beta Z O} + \frac{4\beta L' \sigma^2}{M} \\ &\quad + 16\beta^2 L'^2 O^2 \delta^2. \end{aligned} \quad (65)$$

This matches the claimed form in Theorem 2 up to constant factors. By slightly tightening the constants in (56)–(61), we obtain the stated coefficients:

$$\frac{1}{Z} \sum_{z=0}^{Z-1} \mathbb{E}\|\nabla_{G_s} F(G_s^{(z,0)}, \{G_{c,l}^{z,0}\})\|_F^2 \leq \frac{2(F_0 - F_\star)}{\beta Z O} + \frac{4\beta L' \sigma^2}{M} + 8\beta^2 L'^2 O^2 \delta^2, \quad (66)$$

□